[3]Magness, D., Robinson, O., and Rockwell, D., "Control of Leading-Edge Vortices on a Delta Wing," AIAA Paper 89-0999, Tempe, AZ, March 1989.

[4]Brandon, J. M., and Shah, G. H., "Unsteady Aerodynamic Characteristics of a Fighter Model Undergoing Large Amplitude Pitching Motions at High Angles of Attack," AIAA Paper 90-0309, Reno, NV, Jan. 1990.

[5]DelFrate, J. H., and Zuniga, F. A., "In-Flight Flow Field Analysis on the NASA F-18 High Alpha Research Vehicle with Comparisons to Ground Facility Data," AIAA Paper 90-0231, Reno, NV, Jan. 1990. (See also NASA TM 4193, May 1990).

[6]Hebbar, S. K., Platzer, M. F., Park, S. N., and Cavazos, O. V., "A Dynamic Flow Visualization Study of a Two-Percent F/A-18 Fighter Aircraft Model at High Angles of Attack," NASA High-Angle-of-Attack Technology Conference, Oct.–Nov. 1990, Hampton, VA. (Also to appear as NASA CP, 1991.)

[7]Cavazos, O. V., "A Dynamic Flow Visualization Study of LEX-Generated Vortices on a Scale Model of a F/A-18 Fighter Aircraft at High Angles of Attack," Master's Thesis, Naval Postgraduate School, Monterey, CA, June 1990.

[8] Hebbar, S. K., Platzer, M. F., and Cavazos, O. V., "A Water Tunnel Investigation of the Effects of Pitch Rate and Yaw on LEX-Generated Vortices of an F/A-18 Fighter Aircraft Model," AIAA Paper 91-0280, Reno, NV, Jan. 1991.

Thin-Airfoil Correction for Panel Methods

J. Carter* and P. S. Jackson†
University of Auckland, Auckland, New Zealand

Introduction

THE so-called "panel" methods for calculating potential flows over lifting bodies begin with an appropriate form of Green's theorem, which requires the evaluation over the body surface of integrals involving the potential ϕ. This is done by redefining the surface as a series of panels, with ϕ taking an assumed distribution on each panel, which is sufficiently simple for the integral over the panel to be carried out analytically. The basis of the method may be found in Hunt[1] or Moran.[2] For thick airfoils and other bodies without sharp edges, the potential and its gradients are well-behaved everywhere, and the panel methods give excellent predictions of lift and induced drag. However for thin bodies, or flows that involve a sharp edge at which the Kutta condition is not satisfied, singularities appear at the sharp edges and the method becomes less well behaved. The purpose of this note is to point out that a simple modification to a conventional panel method for such problems accounts for the main effect of this singularity and produces a significant increase in accuracy.

Accounting for the Edge Singularity

Most panel methods assume a fixed value of ϕ on each of a number of surface panels, and find the local surface velocities from the local gradients of the potential. The gradients are found either numerically or by fitting a different assumed form for ϕ over the panel of interest and its neighbors. The following example is worked out for a thin two-dimensional airfoil having a sharp edge at $x = 0$. Assuming a quadratic form, the expression

$$\phi = A + Bx + Cx^2 \tag{1}$$

is fitted to the discrete values of ϕ already calculated for the nth panel and its two neighbors, using values for x at the panel control points. The velocity jump at the panel control point x_{nc} is then calculated using

$$\Delta v_n = B + 2Cx_{nc}$$

The loading is assumed constant over the element, and as it is proportional to the velocity jump the final steps are to multiply each control point velocity by the panel area A_n to give a panel force

$$f_n = A_n \Delta v_n$$

and to then sum the force components over the panels.

The primary source of inaccuracy in this process is easily demonstrated, using the known distribution for the jump in potential function near the sharp leading edge of two-dimensional airfoil

$$\phi = x^{1/2} \tag{2}$$

The airfoil surface is divided into panels of width A_n, with control points at the center of each element. Equation (2) is used to evaluate ϕ at the control points, and then the above procedure is used to find the velocity and force on the first four elements from the leading edge. The exact results for each element are also readily obtained from Eq. (2).

The results of this process are shown in Table 1 for the case of uniform panel size (unit width) when, for example, the quadratic fit of Eq. (1) to Eq. (2) over the first three elements is

$$\phi = 0.387 + 0.680x - 0.081x^2$$

It is clear from the table that the largest error by far occurs on the first panel (as expected, because the singularity is at the origin), and that on subsequent panels, the quadratic approximation gives quite good answers. The usual methods of improving the accuracy of the method are either to use higher panel density or, more properly, by moving the control points away from the panel centers in the manner described by James,[3] Guermond,[4] and others. The remedy proposed here is to account for the presence of the singularity in the leading-edge panel only, by fitting an alternative expression to the potential in that neighborhood that is derived from the exact solution for the flow around a flat plate. Specifically, Eq. (1) is replaced by

$$\phi = x^{1/2}(A + Bx) + C \tag{3}$$

for the leading-edge element, and the velocity at the control point by

$$\Delta v_1 = \frac{(A + Bx_{1c})}{\sqrt{x_{1c}}}$$

(rather than the exact expression, which would use $0.5A + 1.5Bx_{1c}$) so that when this is multiplied by the panel length, the resulting expression for the load corresponds to the correct value, as derived from Eq. (3). For the special case used as an example, this assumed form for the potential fits exactly, thus in Table 1 the estimated values of velocity and loading would be replaced by their exact values for the first element, with those for the remaining elements remaining unchanged. The estimate of total load is significantly improved as a result.

Table 1 Estimated velocity and loading near a sharp edge (uniform panels)

Element n	1	2	3	4
x_{nc}	0.5	1.5	2.5	3.5
Δv_n	0.599	0.437	0.323	0.270
Exact Δv	0.707	0.408	0.316	0.267
f_n	0.599	0.437	0.323	0.270
Exact loading	1.000	0.414	0.317	0.267

Received July 27, 1991; accepted for publication Aug. 1, 1991.

*Research Fellow, Yacht Research Unit.
†Professor, Department of Mechanical Engineering.

An added bonus of this approach is that the strength of the first term in Eq. (3) may readily be used to find the leading- or side-edge suction on a sharp edge, and several previous authors have used a similar expression for this purpose (but not for correcting the pressure force). It is also exactly the calculation required to use the Polhamus[5] expression for vortex lift due to edge separation, although, in that case, the above loading correction to the first panel should not be made because the edge singularity is absent from the physical flow.

Table 2 repeats this analysis for element spacing which is equivalent to the well-known "cosine" spacing, when respective panel sizes are 1/4, 4/4, 9/4, 16/4, and 25/4 (with the division by 4 used to make the first four panels occupy a length of four units as before). It may be seen that by itself this panel spacing does not improve the inherent accuracy. Errors in loading are reduced only because the panels with the largest errors are reduced in size, and not because the singularity is being properly accounted for (which, as noted above, requires the control points to move away from the panel centers). However, as noted below, the cosine spacing greatly improves the estimates of the coefficient A and, subsequently, of the induced drag. For bodies with swept edges, it is important to find the gradient of the potential normal to the edge in order to find the singularity strength—otherwise, the corrections suggested above are applied as described.

Accuracy of the Correction

In order to assess the accuracy of the proposed scheme and to find its convergence rate, calculations of lift and drag have been performed on simple planforms using a panel method based on that described by Maskew.[6] These forces have been found in four ways—two use the pressure integration described above, first without (PI), and then with (CPI) the proposed correction to the edge panels. The third ($CPI + S$) adds to the second the forces due to leading-edge suction. In the fourth, the forces given are those acting on a lifting line that terminates the trailing wake well downstream. Because the resulting lifting surface, wake, and lifting line is a finite three-dimensional body with no shed vorticity, the total force on the body must vanish. Because there is no force on the wake (not quite correct here, as a plane fixed wake is assumed), the force on the lifting line (LL) must equal that on the lifting surface (with its leading-edge suction included).

Results are presented here only for a rectangular wing of aspect ratio 2 at 10-deg incidence using cosine panel spacing, but the conclusions have been confirmed for a range of other wing shapes. Figure 1 shows the lift coefficients obtained with N chordwise and $2N$ spanwise panels of uniform size. As expected all the methods show $1/N$ convergence and seem to be converging to the same value. However when the panel density is coarse, $CPI + S$ gives results much closer to the limiting lift than either of the other two methods. Adding the leading-edge suction term makes little difference to the lift, and so CPI has been omitted for clarity.

Figure 2 shows the predicted drag coefficients, which are very sensitive to the accuracy of the leading-edge suction term. Because the pressure integration alone does not include leading-edge suction, it gives hopelessly unreliable results. With the suction included, the surface force and lifting line force show very good agreement. The modification suggested in this note primarily affects the normal force of the leading element, and thus has little influence on the drag.

Table 2 Estimated velocity and loading (cosine spacing)

Element n	1	2	3	4
x_{nc}	0.125	0.625	1.625	3.125
Δv_n	1.00	0.743	0.421	0.295
Exact Δv	1.414	0.632	0.461	0.283
f_n	0.250	0.557	0.527	0.516
Exact loading	0.500	0.500	0.500	0.500

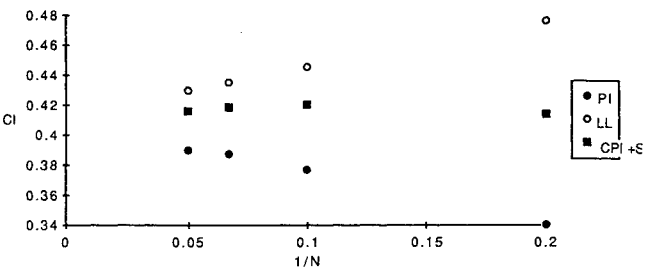

Fig. 1 Convergence of lift coefficient (rectangular plate with regular spacing).

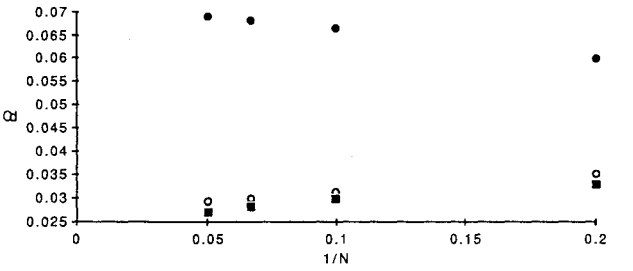

Fig. 2 Convergence of drag coefficient (rectangular plate).

Table 3 Potential and vortex lift factors for a rectangular wing

	Kv		
Kp	Leading edge	Side edge	Method
2.48	1.50	1.58	Lan[7]
2.46	1.55	1.45	Hardy & Fiddes[8]
2.41	1.51	1.41	Present paper

Finally, Table 3 shows the results for the potential lift and vortex lift parameters (as defined by Polhamus) for the leading and side edges of a rectangular plate. These compare very well with those obtained by Lan[7] using the QCM method, and by Hardy and Fiddes[8] using a panel method.

Conclusions

The correction proposed to the calculation of pressure forces on a sharp-edged body has been shown to improve significantly the estimates of total force, lift in particular. It is easily incorporated into standard panel methods without compromising their usual panel and control point configurations, and involves only a small modification to a common procedure for estimating leading-edge suction forces. Most importantly, it shows excellent agreement between the drag force calculated from forces acting directly on the body and those inferred from a lifting line that terminates the wake, thus allowing a simple self-checking procedure for the drag.

References

[1]Hunt, B. "The Mathematical Basis and Numerical Principles of the Boundary Integral Method for Incompressible Potential Flow over Three-Dimensional Aerodynamic Configurations," *Numerical Methods in Applied Fluid Mechanics*, Academic Press, New York, 1982, pp. 49–135.

[2]Moran, J. *An Introduction to Theoretical and Computational Aerodynamics*, Wiley, New York, 1984.

[3]James, R. M., "On the Remarkable Accuracy of the Vortex Lattice Method," *Computer Methods in Applied Mechanics and Engineering*, Vol. 1, 1972, pp. 59–79.

[4]Guermond, J-L., "Collocation Methods and Lifting Surfaces," *European Journal of Mechanics, B: Fluids*, Vol. 8, No. 4, 1989, 283–305.

[5]Polhamus, E. C., "A Concept of Vortex Lift of Sharp-Edged Delta Wings Based on the Leading-Edge Suction Analogy," NASA TN D-3767, 1966.

[6]Maskew, B., "Program VSAERO—Theory Document," Ana-

lytical Methods Inc., Washington, DC, 1982.
[7]Lan, C. E., and S. C. Mehrotra, "An Improved Woodward's Panel Method for Calculating Leading-Edge and Side-Edge Suction Forces at Subsonic and Supersonic Speeds," NASA CR 3205, 1979.
[8]Hardy, B. C., and S. P. Fiddes, "Prediction of Vortex Lift on Non-Planar Wings by the Leading-Edge Suction Analogy," *Aeronautical Journal*, Vol. 92, No. 914, 1988, 154–164.

Wing Mass Formula for Subsonic Aircraft

Sergei V. Udin* and William J. Anderson†
University of Michigan, Ann Arbor, Michigan 48109

Description

MOST wing mass formulae[1,2] are based on statistical information. As a consequence, these formulae usually have good accuracy only on a restricted set of wing data. A theoretical wing mass derivation based on a simplified concept model of a wing is presented in Ref. 3. This method takes into consideration all the details of the aircraft wing, including complicated geometry and concentrated loads, such as the engines. Formulae to estimate mass due to swept moment, mass due to twist moment, and mass due to shear are presented below. The mass of other wing components, which total about 30% of the wing mass, can be estimated by known methods.[1,4] The reader is referred to a complete and detailed derivation in Ref. 5.

The geometry of a subsonic aircraft wing with span b is shown in Fig. 1. We define the *inboard wing* as the part of the wing between the fuselage joints. It is assumed that the inboard wing section is not tapered and not swept. The *midboard wing* is the part of the wing between the fuselage joint and the sweep joint. The *outboard wing* lies between the sweep joint and the wing tip. We consider that the aircraft has no inboard wing concentrated loads, has n_m i-numbered midboard wing concentrated loads, and has n_o j-numbered outboard wing concentrated loads. The relative mass of each load is $\frac{1}{2}m_c^i$ or $\frac{1}{2}m_c^j$ (i.e., m_c^i or m_c^j is the mass of both symmetric loads located in both parts of the wing). The relative coordinate of a concentrated load (absolute Z^i or Z^j coordinate divided by half-span) is z_c^i or z_c^j.

The estimated relative mass of the wing structure is

$$m_w = k_{tm}(m_M + m_Q) + m_{\text{rib}} + m_{\text{ail}} + m_{\text{sk}} + m_{\text{flap}} \quad (1)$$

The formulae to estimate relative masses of ribs m_{rib}, ailerons m_{ail}, load-free skin m_{sk}, and flaps m_{flap} are presented in Refs. 1, 2, and 4. The twist moment factor k_{tm} is

$$k_{tm} = 1 + \frac{0.015\sqrt{A}(1 + 2\lambda_t)}{(1 + \lambda_t)\cos\Lambda} \quad (2)$$

where A is the aspect ratio, λ_t is the taper ratio to wing tip (wing tip chord divided by wing root chord), and Λ is the half-chord wing sweep.

Received May 6, 1991; accepted for publication May 28, 1991.

*Visiting Research Scholar, Aerospace Engineering Department. Permanent affiliation: Graduate Student, Moscow Aviation Institute, Moscow, Russia.
†Professor of Aerospace Engineering. Senior Member AIAA.

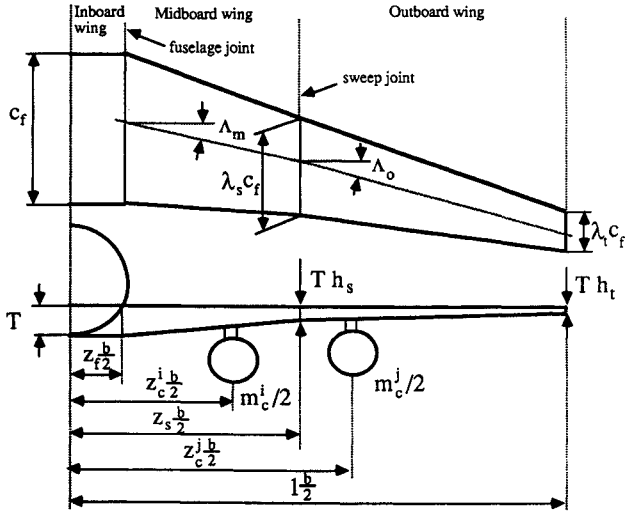

Fig. 1 Wing geometry.

The relative masses of structure counteracting the bending moment and shear are

$$m_M = \left(\frac{\rho_{\text{lower}}}{\sigma_{\text{act lower}}} + \frac{\rho_{\text{upper}}}{\sigma_{\text{act upper}}}\right)\frac{Ag_d a\mu E_T}{4pT}(K_{M_i} + K_{M_m} + K_{M_o}); \quad m_Q = 0.1\, m_M \quad (3)$$

where ρ_{lower} and ρ_{upper} are densities of lower and upper panel structural materials, g_d is the design overload factor, a is gravitational acceleration, μ is the mass of the aircraft, and p is wing loading. The approximate value of effective airfoil thickness coefficient E_T is

$$E_T \approx 1.1\left(\frac{4T_2}{T_1 + 2T_2 + T_3}\right)^2 \approx 1.2 \cdots 1.4 \quad (4)$$

where T_1 is the first spar height, T_2 is the maximum airfoil height, and T_3 is the most rearward spar height. The values of actual stresses averaged over the lower panel volume $\sigma_{\text{act lower}}$ and the values of actual stresses averaged over the upper panel volume $\sigma_{\text{act upper}}$ can be obtained from the statistics of an aircraft with approximately the same mass, size, and manufacturing quality. These values also can be estimated as

$$\sigma_{\text{act lower}} = \frac{\sigma_{u\,\text{lower}}}{k_{sl\,\text{lower}}k_{\text{man}}}; \qquad \sigma_{\text{act upper}} = \frac{\sigma_{u\,\text{upper}}}{k_{sl\,\text{upper}}k_{\text{man}}}, \quad (5)$$

where the coefficient $k_{sl\,\text{lower}}$ is the lower panel ultimate stress $\sigma_{u\,\text{lower}}$ divided by the permissible fatigue lower panel stress, $k_{sl\,\text{upper}}$ is upper panel ultimate stress $\sigma_{u\,\text{upper}}$ divided by the permissible fatique upper panel stress and the manufacturing coefficient k_{man} has expert value within bounds presented in Table 1. The value of k_{man} decreases when the dimensions and mass of aircraft are increased. If the absolute root wing thickness T does not exist, it can be inferred from the overall geometry as

$$T = \frac{2t_r}{(\lambda_t + \lambda_s)(1 - z_s) + (1 + \lambda_s)(z_s - z_f) + 2z_f}\sqrt{\frac{\mu}{pA}} \quad (6)$$

where t_r is the root relative thickness; λ_s is the taper ratio to the sweep joint (chord at sweep joint divided by root chord); z_s is the relative coordinate of sweep joint; and z_f is the relative coordinate of fuselage joint. The coefficients K_{M_o}, K_{M_m}, and K_{M_i} in Eq. (3) are